



NRC Publications Archive Archives des publications du CNRC

Flexible ultrasonic transducers for structural health monitoring of metals and composites

Kobayashi, Makiko; Wu, K. -T.; Shih, J. -L.; Jen, C. -K.; Kruger, S. E.

This publication could be one of several versions: author's original, accepted manuscript or the publisher's version. / La version de cette publication peut être l'une des suivantes : la version prépublication de l'auteur, la version acceptée du manuscrit ou la version de l'éditeur.

For the publisher's version, please access the DOI link below. / Pour consulter la version de l'éditeur, utilisez le lien DOI ci-dessous.

Publisher's version / Version de l'éditeur:

<https://doi.org/10.1117/12.848863>

Proceedings of SPIE, 7648, 2010-03-07

NRC Publications Record / Notice d'Archives des publications de CNRC:

<https://nrc-publications.canada.ca/eng/view/object/?id=8d043598-2a6c-4e64-bd66-fe066faa0f16>

<https://publications-cnrc.canada.ca/fra/voir/objet/?id=8d043598-2a6c-4e64-bd66-fe066faa0f16>

Access and use of this website and the material on it are subject to the Terms and Conditions set forth at

<https://nrc-publications.canada.ca/eng/copyright>

READ THESE TERMS AND CONDITIONS CAREFULLY BEFORE USING THIS WEBSITE.

L'accès à ce site Web et l'utilisation de son contenu sont assujettis aux conditions présentées dans le site

<https://publications-cnrc.canada.ca/fra/droits>

LISEZ CES CONDITIONS ATTENTIVEMENT AVANT D'UTILISER CE SITE WEB.

Questions? Contact the NRC Publications Archive team at

PublicationsArchive-ArchivesPublications@nrc-cnrc.gc.ca. If you wish to email the authors directly, please see the first page of the publication for their contact information.

Vous avez des questions? Nous pouvons vous aider. Pour communiquer directement avec un auteur, consultez la première page de la revue dans laquelle son article a été publié afin de trouver ses coordonnées. Si vous n'arrivez pas à les repérer, communiquez avec nous à PublicationsArchive-ArchivesPublications@nrc-cnrc.gc.ca.



Flexible Ultrasonic Transducers for Structural Health Monitoring of Metals and Composites

M. Kobayashi^a, K.-T. Wu^b, J.-L. Shih^b, C.-K. Jen^a and S. E. Kruger^a

^aIndustrial Materials Institute, National Research Council of Canada, 75 Blvd. de Mortagne,
Boucherville, Quebec J4B 6Y4, Canada;

^bDepartment of Electrical and Computer Engineering, McGill University, 3480 University Street,
Montreal, Quebec H3A 2A7, Canada;

ABSTRACT

Flexible ultrasonic transducers (FUTs) which have the on-site installation capability are presented for the non-destructive evaluation (NDE) and structural health monitoring (SHM) purposes. These FUTs consist of 75 μm thick titanium membrane, thick ($> 70 \mu\text{m}$) thick piezoelectric lead-zirconate-titanate (PZT) composite (PZT-c) films and thin ($< 5 \mu\text{m}$) thick top electrodes. The PZT-c films are made by a sol-gel spray technique. Such FUT has been glued onto a steel pipe of 101 mm in diameter and 4.5 mm in wall thickness and operated up to 200°C. The glue served as high temperature ultrasonic couplant between the FUT and the external surface of the pipe. The estimated pipe thickness measurement accuracy at 200°C is 34 μm . FUTs also were glued onto the end edge of 2 mm thick aluminum (Al) plates to generate and receive predominantly symmetrical and shear-horizontal (SH) plate acoustic waves (PAWs) to detect simulated line defects at temperature up to 100°C. FUTs glued onto a graphite/epoxy (Gr/Ep) composite are also used for the detection of artificial disbonds. An induction type non-contact method for the evaluation of Al plates and Gr/Ep composites using FUTs is also demonstrated.

Keywords: Flexible ultrasonic transducer, structural health monitoring, high temperature ultrasonic measurement, nondestructive testing

1. INTRODUCTION

NDE of pipes in nuclear and fossil fuel power plants¹⁻⁴, chemical and petroleum plants^{1, 2} has become an increasingly important element in the improvement of safety and in the extension of a structure's life span. SHM⁵⁻⁹ which may provide continuous NDE of pipes or their health conditions has also drawn much attention recently. Ultrasonic techniques are frequently used for these NDE and SHM purposes because of their subsurface inspection capabilities, fast inspection speeds, simplicity and ease of operation. In these applications, ultrasonic transducers (UTs) may need to be made directly in contact with structures that have surfaces with different curvatures and must also be able to operate at elevated temperatures^{3, 4, 10-13}. Also Civil and military aircraft operators around the world have incurred rising maintenance costs due to their aging fleets. They are seeking ways to reduce the fleets maintenance cost while still meeting airworthiness requirements. SHM is potentially a cost effective emerging area of technology that enables condition-based maintenance in-lieu of the traditional schedule-based NDE. For aerospace structures, composite materials, such as Gr/Ep laminates, are becoming the materials of choice because of the high strength to weight ratio. SHM^{8, 9} and NDE technologies^{1, 2} for these Gr/Ep composites are being developed to enable condition-based maintenance for cost-effective increased safety and eco-efficient designs.

In ultrasonic NDE and SHM applications, ultrasonic transducers (UTs) may need to be made directly in contact with structures that have surfaces with different curvatures and/or be able to operate at elevated temperatures. However, conventional UTs having rigid flat end surfaces may in general show poor performance and therefore may not be readily suitable for the inspection of curved surface such as pipes. The poor signal-to-noise ratio (SNR) may in part come from the fact that the contacting area is a narrow line allowing only a small portion of the available ultrasonic energy to be transmitted into the pipe. Different thicknesses in gel couplant that are present in the gap area between the UT flat end surface and the curved surface of the pipe cause the areas other than this narrow contact line of the UT to generate

unwanted noises. It also means that such unwanted noises are induced by the spatial spread of the UT excitation. Flexible UTs (FUTs)¹³⁻¹⁹ are therefore more suitable under such conditions because they ensure their own self-alignment to the object's surface even in the case of a complex geometry so that the transmitted ultrasonic energy may be maximized and noise may be minimized to improve SNR for NDE and SHM purposes. FUTs have been made of PVDF^{14, 15}, PZT 1-3 composites^{16, 17} and PZT fibers incorporated into composites¹⁸⁻¹⁹. In this study the fabrication of FUTs is based on a sol-gel spray technique^{12, 13, 19, 20}. Titanium (Ti) membranes of 75 μm thick will be used as the substrate. The center operation frequency of these FUTs serve as longitudinal L wave UTs will be around 9 MHz during the ultrasonic measurements. All measurements will be carried out in pulse/echo mode.

It is known that plate acoustic waves (PAW)^{7, 21, 22} can propagate in a distance of more than tens or hundreds of cm in metal plates such as aluminum (Al) or steel. PAWs can be excited and received by bulk wave transducers with a wedge^{21, 22} and interdigital transducers²². They are excellent candidates for global (large area) damage monitoring of metallic plates⁷. In this study FUTs will be glued at the end edges of metallic plates with proper mode conversion angles^{22, 23} and directions to generate and receive predominantly symmetric and shear-horizontal (SH) PAWs for line crack detection demonstration. This study will further present an induction type non-contact method^{24, 25} for the interrogation of the metal and Gr/Ep composite samples using FUTs. Such non-contact technique may be desired for SHM and NDE of rotating components.

2. FABRICATION AND ULTRASONIC PERFORMANCES OF FUTS AS L WAVE UT

FUTs to be presented use thick film fabrication technology and the substrates are 75 μm thick Ti membranes. In this study the fabrication of the FUT based on a sol-gel spray technique consists of six main steps^{12, 13, 19}: (1) preparing a high dielectric constant PZT solution, (2) ball milling the piezoelectric PZT powders in a PZT solution to submicron sizes, (3) sensor spraying using slurries from steps (1) and (2) to produce a film with thicknesses of between 5 and 20 μm , (4) heat treating to produce a solid PZT composite (PZT-c) thick film and the highest temperature for treatment is 650°C, (5) Corona poling to obtain piezoelectricity, and (6) silver paste painting for depositing electrical connections. Steps (3) and (4) are performed multiple times to produce optimal film thicknesses for specified ultrasonic operating frequencies. In this investigation, steps (4) and (5) are significantly different from the FUT processes presented in^{12, 13, 19}. Here a rapid thermal annealing like process²⁶⁻²⁸ was used for the thermal treatment. The main advantage of rapid thermal annealing is to limit the eventual degradation of the film-substrate interface such as through inter-diffusion of lead and also to improve the crystallization behavior of the piezoelectric film. The short annealing time also helps to avoid the growth of an oxidation layer between the Ti membrane and the PZT-c film. Oxidation layers reduce the electrical conductivity of Ti, thereby decreasing the ultrasonic performance. The flexibility of the FUTs comes from the thinness of the membrane substrate, the piezoelectric film and the top electrode, as well as from the porosity of the piezoelectric film. The porosity of the piezoelectric PZT-c films, which are controlled during film fabrication, is an important factor to achieve the frequency bandwidth of the FUTS presented in this paper.

2.1. Ultrasonic Measurement of Pipes at 200°C

Fifteen FUTs consisting of a 75 μm thick Ti membrane, a 92 μm thick PZT-c film and a 10 μm thick silver paste was firstly fabricated and shown in Fig. 1. Ti membranes are chosen here to reduce the oxidation during the thermal treatment and they are more flexible than the stainless steel membranes of the same thickness reported in^{13, 19}. One of them, with a modified silver paste top electrode size having a length of 4 mm and a width of 2 mm, was cut and glued onto a steel pipe as shown in Fig. 2a. The glue was cured at 80°C for 90 minutes. The outer diameter (OD) and the wall thickness of the steel pipe were 101 mm and 4.5 mm, respectively. In Fig. 2b ultrasonic pulse/echo measurement at 200°C was taken by the EPOCH LT pulser/receiver (from Olympus-Panametrics, USA) together with two spring electrical contacts, one of which connects to the top silver paste electrode and the other to the bottom electrode, which was the Ti substrate. This particular type of handheld device is used on a daily basis for NDE in industrial settings. It also does not have the functionality of signal averaging and filtering and only displays the raw ultrasonic measurement data. Performance levels achieved and demonstrated on this handheld device with the fabricated FUTs on flat and curved surfaces help to demonstrate the applicability of such FUTs under current industrial SHM and NDE settings. The pulse energy used was 100 volts, the lowest available of the EPOCH LT, and the gain used was 16 dB out of the available 100 dB. Figures 3a and 3b show the measured ultrasonic signals in time and frequency domain, where L^n is the n^{th} trip of the

longitudinal echo (L) through the pipe wall thickness. The center frequency and the 6 dB bandwidth of the L^2 echo were 9.8 MHz and 8.1 MHz respectively. The signal strength at 200 °C is 8 dB weaker than that at room temperature and this 8 dB reduction comes from the ultrasonic loss in glue and steel and the reduced piezoelectric strength of PZT-c film at 200°C. When this FUT is tested with a metal plate, its signal strength is the same as that obtained with a commercial broadband UT which, however, is difficult to be used for pipes at 200°C.

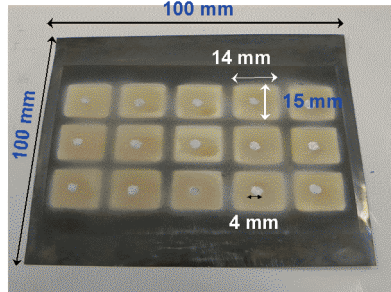


Fig. 1. Fifteen FUTs coated onto 75 μm thick Ti membrane. The PZT-c film thickness is 92 μm . Top silver electrodes are made.

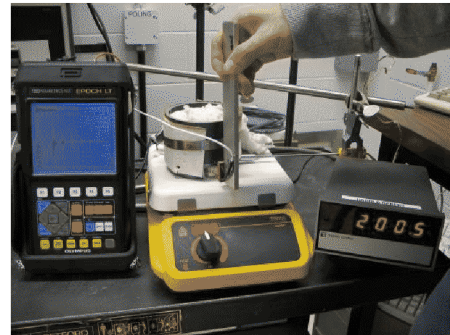
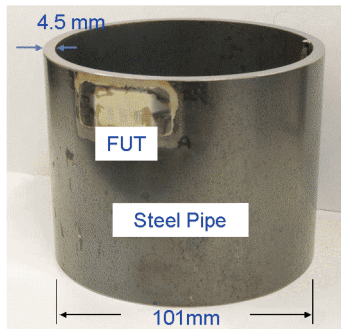


Fig. 2. (a) One FUT shown in Fig. 1 glued to a steel pipe with an O.D. of 101 mm and a thickness of 4.5 mm, (b) ultrasonic measurement at 200°C.

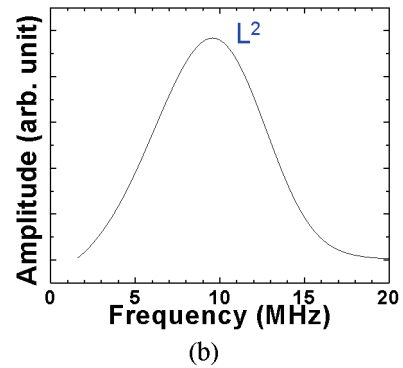
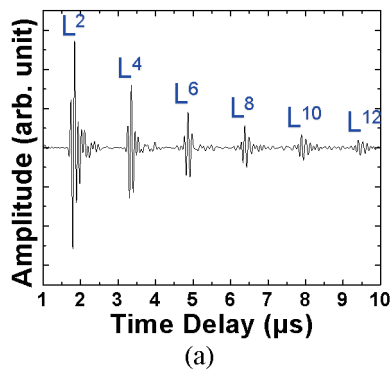


Fig. 3. Ultrasonic signals obtained with the experimental setup shown in Fig. 2b; (a) in time domain and (b) L^2 in frequency domain.

2.2. Thickness Measurement Accuracy at 200°C

Equation (1) (Equation 19 in ²⁹) is used here for the estimation of the accuracy in time delay measurement and by

extension, in the thickness measurement of the steel pipe shown and tested under the conditions presented in Fig. 2b. The equation takes into account jitter and false peak errors that may arise in delay time estimations that are commonly due to noise, finite window lengths and signal decorrelations resulting from the experimental setup and/or the imperfections in the transducers.

$$\sigma(\Delta t - \Delta t') \geq \sqrt{\frac{3}{2f_0^3 \pi^2 T (B^3 + 12B)} \left(\frac{1}{\rho^2} \left(1 + \frac{1}{SNR_1^2} \right) \left(1 + \frac{1}{SNR_2^2} \right) - 1 \right)} \quad (1)$$

In this equation, f_0 is the center frequency, T is the time window length for the selection of L^2 and L^4 in Fig. 3a that is required for the cross correlation measurement, B is the fractional bandwidth of the signal, which is the ratio of the signal bandwidth over f_0 , ρ is the correlation coefficient, SNR_1 and SNR_2 are the SNR of the L^2 and L^4 echo respectively, and $\sigma(\Delta t - \Delta t')$ is the standard deviation of the measured time delay (Δt being the true time delay and $\Delta t'$, the measured time delay). Using Equation 1 and the parameters tabulated in Table 1, which characterize this particular brazed FUT, the calculated $\sigma(\Delta t - \Delta t')$ was 2.61 ns.

Table 1: Parameters for Equation 1 and digitization resolution

Parameters	Values for the FUT glued on steel pipe
f_0	9.8 MHz
T	0.32 μ s
B	0.82
ρ	0.94
SNR_1	15 dB
SNR_2	15 dB
$\sigma(\Delta t - \Delta t')$	2.61 ns
Digitization resolution (100 MHz) including interpolation	2 ns
Total time delay uncertainty	4.61 ns
V_L	5755 m/s
Thickness measurement accuracy	13.3 μ m

Since a sampling rate of 100 MHz was used in the experiment, with the use of the cross correlation method and taking into account interpolation³⁰, the time measurement error, which may be additionally introduced, was estimated to be at an upper limit of 2 ns. The total uncertainty in time delay measurement was therefore estimated at 4.61 ns. Since the measured longitudinal velocity V_L in the steel pipe using the pulse-echo technique at 200°C was 5755 m/s, the best possible thickness measurement accuracy achievable on this 4.5 mm thick pipe was 13.3 μ m in pulse-echo mode at 200°C. If the sampling rate is increased to more than 100 MS/s, improved thickness measurement accuracy may be obtained; however this result established according to equation (1) demonstrates that at such a sampling rate, the fabricated FUTs centered at 10.8 MHz have a SNR and a bandwidth that are sufficient for thickness measurements of such steel pipes of 4.5 mm thick at 200°C.

3. ULTRASONIC PERFORMANCES OF FUTS AS PAW UTS

Integrated UTs (IUTs) have been directly deposited onto the edges of Al plates of 2 mm to 6 mm thick to excite and detect the symmetric, anti-symmetric and SH PAWs and operated up to 150°C¹⁵. They do not need couplant such as glue. However, since the substrates such as Al plate may not be allowed to be heat treated up to 650°C, the signal strength of the IUTs may not be strong due to the low heat treatment temperatures. Here, the purpose is to demonstrate the on-site installation merit of FUT together with the glue of which the good ultrasonic performance has been illustrated in Section 2. In this study Al plates of 406 mm by 50.8 mm by 2 mm thick will be used for the demonstration.

3.1. Symmetric PAW

Firstly a FUT is glued onto the end area of 50.8 mm by 2 mm of the Al plate as shown in Fig. 4. Figure 5 is a zoom picture of this FUT and the thickness of the PZT-c film of this FUT is 99 μm . The top electrode has a height of 38 mm and a width of 2 mm, which define this FUT active area. Figures 4 and 5 also demonstrate that the dimensions of FUTs presented in this study may be changed very easily. The glue which is different from the one applied in Section 2.1 was cured at room temperature for 24 hours. This FUT generates and detects surface displacements predominantly oriented along the length direction of the plate. In order to demonstrate the global NDE and SHM capability of the PAW two artificial line defects, D1 and D2 with 1 mm depth and 1 mm width were made onto the Al plate shown in Fig. 4. D1 and D2 are 25.4 mm and 50.8 mm long, respectively.

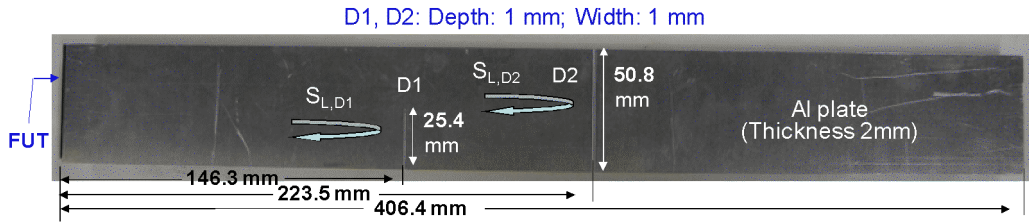


Fig.4. One FUT was glued and two artificial line defects, D1 and D2 were made onto a 2 mm thick Al plate for the demonstration of global NDE capability of PAW.

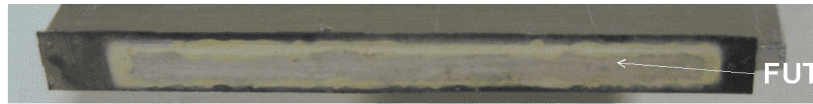


Fig. 5. Zoomed FUT shown in Fig. 4.

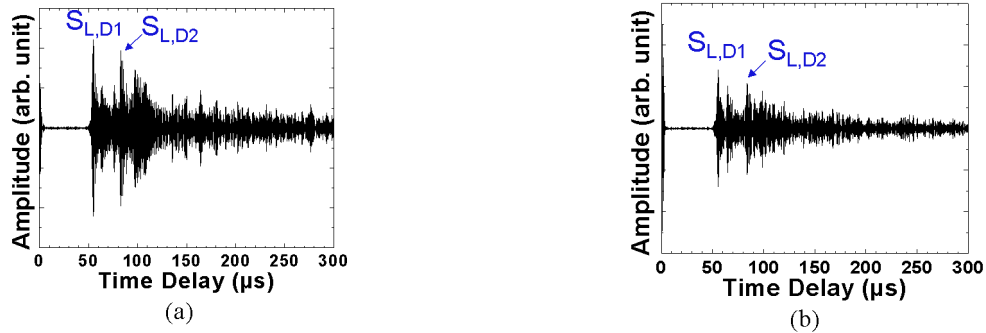


Fig. 6 Symmetrical PAW signals detecting two artificial line defects, D1 and D2 in a 2 mm thick Al plate shown in Fig. 4 at (a) room temperature and (b) 100°C.

Figures 6a and 6b show the measured ultrasonic signals generated and received by the FUT at room temperature and 100°C, respectively. The subscripts D1 and D2 of the $S_{L,D1}$ and $S_{L,D2}$ echoes denotes the 1st round trip reflection from the FUT location to the defects D1 and D2, respectively. The signal strength of e.g. the echo $S_{L,D1}$ at 100°C is 7.5 dB less than that at room temperature. The center frequency and bandwidth of the $S_{L,D1}$ echo at 100°C are 6.5 MHz and 0.5 MHz, respectively. It means that $S_{L,D1}$ has traveled a total distance of 292 mm. The group velocity of the $S_{L,D1}$ echo at the leading edge was about 5462 m/s which is slower than that of the measured through Al plate thickness L wave velocity, $V_L = 6364$ m/s. In ²⁵ the calculated phase and group velocities versus the product of PAW frequency, f , and plate thickness, h , curves for the first few symmetrical (S) and anti-symmetrical (a) PAW modes of the Al plate shown in

Fig.4 can be found. Figure 6 implies that $S_{L,D1}$ consists of many lower order symmetrical modes. From the measured group velocity of 5462 m/s and the calculated dispersion curves shown in ²⁵ it is believed that the main symmetrical mode contribution to the $S_{L,D1}$ signal would be S^4 , the 4th order of symmetrical PAW mode. At room temperature the strength of the $S_{L,D1}$ signal is 15 dB stronger than that generated and received by IUT reported in ²⁵.

3.2. SH PAW

A FUT is also glued at the side edge near the end of a 2 mm thick Al plate with a length of 406.4 mm and a width of 50.8 mm as shown in Fig. 7. The same glue used in Section 3.1 was applied. Two artificial line defects, D1' and D2' with 1 mm depth and 1 mm width were also made onto this Al plate, and D1' and D2' had a length of 25.4 mm and 50.8 mm, respectively. Using mode conversion^{22,23} SH PAW may be predominantly excited and received²⁵. The top rectangular electrode of the FUT shown in Fig. 8 has a height of 2 mm and a width of 25 mm, which define this FUT active area. For this configuration symmetrical PAW traveled nearly 25.4 mm and then converted to SH PAW modes and vice versa. For this configuration the chosen mode conversion angle using the analogy of L to S wave was 61.7° which was calculated using the phase matching between measured extension mode velocity^{21, 22} and the S wave velocity of the Al plate²⁵.

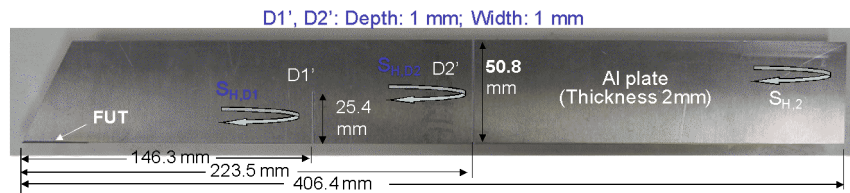


Fig. 7. One FUT was glued and two artificial line defects, D1 and D2 were made onto a 2 mm thick Al plate for the demonstration of global NDE capability of PAW.

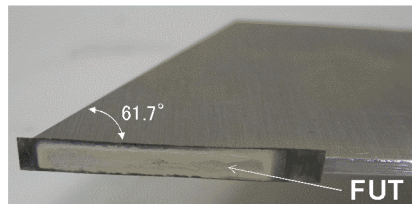


Fig. 8. Zoomed FUT shown in Fig. 7.

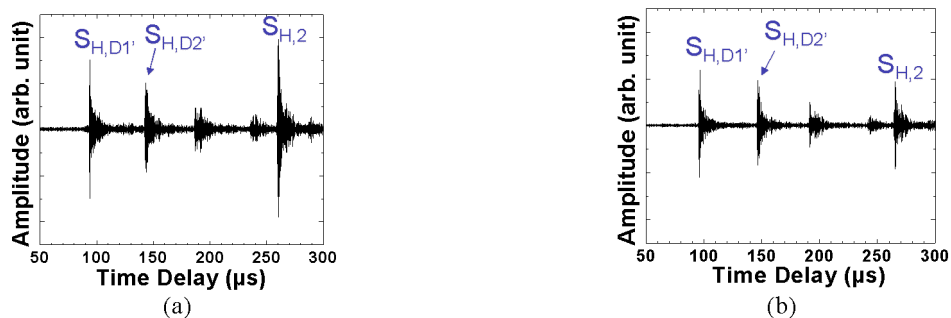


Fig. 9 SH PAW signals detecting two artificial line defects, D1' and D2' in a 2 mm thick Al plate shown in Fig. 7 at (a) room temperature and (b) 100°C.

The measured predominant SH PAW signals at room temperature and 100°C are shown in Figs. 9a and 9b, respectively. The signal strength of the echo $S_{H,D1'}$ at 100°C, for example, is 2.3 dB less than that at room temperature. The $S_{H,D1'}$ and $S_{H,D2'}$ are the reflected echoes from the artificial line defects D1' and D2', respectively. The echoes between $S_{H,D2'}$ and $S_{H,2}$ come from the multiple reflections between D1' and D2'. It is demonstrated that

not only SH PAWs can clearly detect the defects D1' and D2' which are 146.3 mm and 223.5 mm away, respectively from the FUT at 100°C, but also travel to the end of the plate and return back to the FUT as indicated by the echo $S_{H,2}$ with good SNR. The center frequency and bandwidth of the $S_{H,D1'}$ echo at 100°C are 7.9 MHz and 5.3 MHz, respectively. The theoretical calculated phase and group velocities versus the product of PAW frequency and plate thickness curves for the first few SH PAW modes of the Al plate shown in Fig. 7 can be also found in ²⁵. Since the group velocities of the first several SH PAW modes are close to the S wave velocity of the Al plate in the range of FUT excitation frequency, the pulse widths of the $S_{H,D1'}$ and $S_{H,D2'}$ are narrower than those of the symmetric PAW $S_{L,D1}$ and $S_{L,D2}$ signal shown in Fig. 6. In Fig. 9, $S_{H,2}$ is the first round trip echo from the FUT to the end of the Al plate. Using the echo $S_{H,2}$ the calculated group velocity is 3136 m/s which is close to the shear wave velocity 3144 m/s of the Al plate, thus $S_{H,D1'}$, $S_{H,D2'}$ and $S_{H,2}$ are predominately SH PAW. Comparing the results in Fig. 9a with those in Fig. 6a one can see that SH PAWs can detect two simulated line defects better than symmetrical PAWs.

4. ULTRASONIC MEASUREMENTS OF GR/EP COMPOSITES

FUTs shown in Fig. 1 can be also used as L wave UTs for the evaluation of Gr/Ep composites. A Gr/Ep composites of 8.3 mm thick with a stacking sequence of $([0/45/0/-45/90/90/-45/0/45/0]) \times 3$ was made for the experiment. Artificial defects consisting of a thin Teflon sheet of 25.4 mm by 25.4 mm have been embedded into this sample during fabrication. Firstly ultrasonic C-scan of this sample in a water immersion tank has been performed. The imaging was carried out by a focused ultrasonic transducer with a center frequency of 7.5 MHz, a focal length of 152.4 mm and a diameter of 19 mm. The scanning step was 0.5 mm in the lateral directions. Figure 10 shows the obtained ultrasonic C-scan image near the Teflon insert region indicated as disbond regions. Then two FUTs similar to the one shown in Fig. 1 with a top electrode area of 4 mm diameter were glued onto the composite onto two locations; one without and one with the disbond as shown in Fig. 11. The glue was cured at room temperature for 24 hours. Since the operation temperature of these composites in aerospace industry normally ranges from -60°C to 100°C, both PZT-c thick film FUT together with the glue shown in Fig. 12 have survived several thermal cycles from -60°C to 100°C.

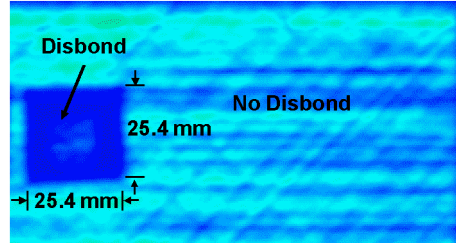


Fig. 10. Ultrasonic C-scan images near the disbond region of the Gr/Ep composite.

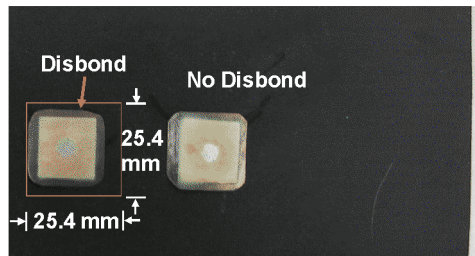


Fig. 11. FUT glued onto the Gr/Ep composite at the location (a) without and (b) with the disbond region.

At room temperature the measured ultrasonic signals obtained by two FUTs shown in Figure 11 are shown in Fig. 12a and 12b, respectively at the location without and with the disbond. L^n is the nth round trip echo through the thickness of the Gr/Ep composite and L_D^n is the nth round trip echo from the FUT to the disbond region. The center frequency and 6 dB bandwidth of the L^1 and L_D^1 echo are 8.9 MHz and 2.5 MHz, 9.4 MHz and 5 MHz, respectively.

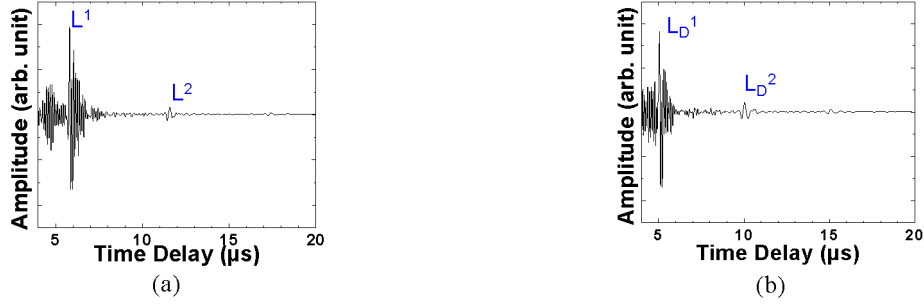


Fig.12 Measured ultrasonic signals in time domain at room temperature at a location (a) without and (b) with disbond using the FUTs shown in Fig. 11.

5. NON-CONTACT APPROACH

In order to achieve NDE and SHM of rotating components non-contact ultrasonic measurements approaches are desired. In this study an induction based method^{24, 25} is used. Here FUTs are replacing the IUTs reported in²⁵. The Al sample shown in Fig. 7 and the Gr/Ep sample with FUTs shown in Fig. 11 are chosen for demonstration purposes. Firstly a flat coil made of thin lacquer wires serves as a main component for induction coupling. The two ends of this coil are connected to the top electrode of the FUT and the Ti membrane which serves as the bottom electrode of the FUT. Directly on top of such coil connected to the FUT there is the other flat coil and the two ends of this coil are connected to the coaxial cable of the pulser/receiver.

Figure 13 shows the measured SH PAW signals along the Al sample shown in Fig. 7 but using the induction based non-contact method. The separation distance between the two coils was 10 mm. The two artificial line defects can be detected. The center frequency and bandwidth of the $S_{H,D1'}$ echo at room temperature are 4.4 MHz and 3.6 MHz, respectively. By comparing the results obtained by non-contact method shown in Figs. 13 with those obtained by the contact method shown in Fig. 9a the receiver gain used was 20 dB higher in non-contact than contact configuration.

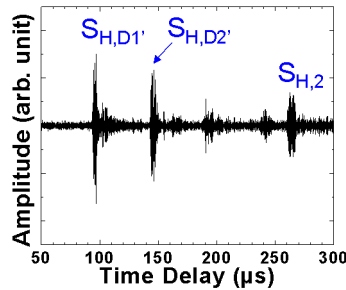


Fig.13. Ultrasonic SH PAW signal in time domain obtained using an FUT shown in Fig.7 with the non-contact configuration at room temperature.

When this non-contact method is applied onto the two FUTs shown in Fig. 11, the measured room temperature ultrasonic signals at the location without and with the disbond are presented in Figures 14(a) and 14(b), respectively. The center frequency and 6 dB bandwidth of the L^1 and L_D^1 echo are 2.9 MHz and 2.1 MHz, 2.9 MHz and 1.8 MHz, respectively. The separation distance between two coils was 10 mm. The ultrasonic signals were 20 dB weaker in non-contact than contact configuration of which the ultrasonic signals are shown in Figures 12(a) and 12(b), respectively. It is noted that the tuning of the electrical impedance matching between the FUTs and the size, diameter and number of turns of coils have not been optimized. Therefore the measured ultrasonic frequency may be significantly affected by the electrical impedance of the coil.

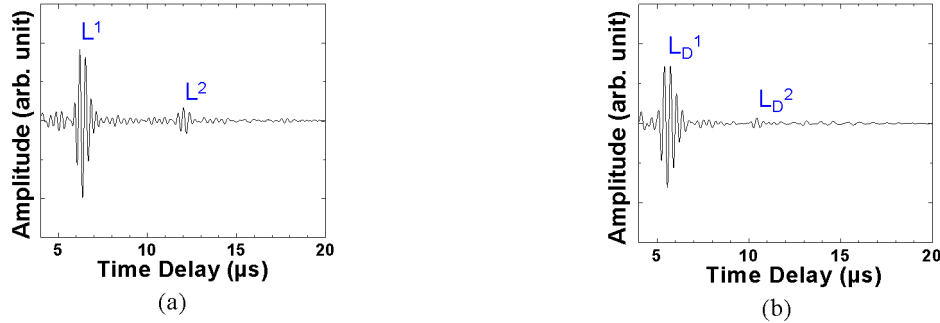


Fig.14 Measured ultrasonic signals in time domain at room temperature at a location (a) without and (b) with disbond using the FUTs shown in Fig. 11 and inductive non-contact method.

6. CONCLUSIONS

FUTs are presented for the non-destructive evaluation (NDE) and structural health monitoring (SHM) purposes. They can be glued on-site and the glue serves as the ultrasonic couplant between the FUT and the object for inspection. These FUTs consist of 75 μm thick Ti membrane, thick ($> 70 \mu\text{m}$) thick piezoelectric PZT-c films and thin ($< 5 \mu\text{m}$) thick top electrodes. The PZT-c films are made by a sol-gel spray technique. Such FUT centered at around 9.8 MHz has been glued onto a steel pipe of 101 mm in diameter and 4.5 mm in wall thickness and operated up to 200°C. The glue served as high temperature ultrasonic couplant between the FUT and the external surface of the pipe. The estimated pipe thickness measurement accuracy at 200°C is 34 μm .

FUTs centered about 6.5 MHz also were glued onto the end edge as shown in Fig. 4 and side edge as shown in Fig. 7 of 2 mm thick aluminum (Al) plates with a length of 406.4 mm and a width of 50.8 mm to generate and receive predominantly symmetrical and shear-horizontal (SH), respectively PAWs at temperature up to 100°C. Two line defects with the dimension of 1 mm in width and 1 mm in depth have the line lengths of 25.4 mm and 50.8 mm in a distance about 146.3 mm and 233.5 mm, respectively away from the FUT location and they can be detected by both symmetrical and SH PAWs. However, the SH PAWs can see these two line defects better than the symmetrical PAWs. FUTs were also glued onto a graphite/epoxy (Gr/Ep) composite of 8.3 mm thick with a stacking sequence of $([0/45/0/-45/90/90/-45/0/45/0])\times 3$. The embedded artificial disbonds can be detected by these FUTs. An induction type non-contact method for the evaluation of Al plates and Gr/Ep composites using FUTs is also demonstrated. Such non-contact technique may be desired for SHM and NDE of rotating components.

ACKNOWLEDGMENT

Financial support from the Natural Sciences and Engineering Research Council of Canada for K.-T. Wu and J.-L. Shih and technical assistance from Jacques Tatibouet and I.-H. Liu are acknowledged.

REFERENCES:

- [1] A.S. Birks, R.E. Green, Jr. and P. McIntire, *Nondestructive Testing Handbook*, 2nd ed., vol.7: Ultrasonic Testing, ASNT, pp.569-587, 1991.
- [2] P.O. Moore, G.L. Workman and D. Kishoni, *Nondestructive Testing Handbook*, 3rd ed., vol.7: Ultrasonic Testing, ASNT, pp.427-474, 2007.
- [3] H. Karasawa, M. Izumi, T. Suzuki, S. Nagai, M. Tamura, and S. Fujimori, "Development of under-sodium three-dimensional visual inspection technique using matrix-arrayed ultrasonic transducer," *Journal of Nuclear Science and Technology*, vol. 37, no. 9, pp. 769-779, 2000.
- [4] S.P. Kelly, I. Atkinson, C. Gregory and K.J. Kirk, "On-line ultrasonic inspection at elevated temperatures", *Proc. IEEE Ultrasonics Symp.*, pp. 904-908, 2007.

- [5] J.-B. Ihn, and F.-K. Chang, "Ultrasonic Non-destructive Evaluation for Structure Health Monitoring: Built-in Diagnostics for Hot-spot Monitoring in Metallic and Composite Structures", Chapter 9 in *Ultrasonic Nondestructive Evaluation Engineering and Biological Material Characterization*, T. Kundu, Ed. Florida: CRC Press, 2003.
- [6] V. Giurgiutiu, [*Structural Health Monitoring with Piezoelectric Wafer Active Sensors*], Elsevier, New York (2007).
- [7] R.P. Dalton, P. Cawley and M.J.S. Lowe, "The potential of guided waves for monitoring large areas of metallic aircraft structure", *J. Nondestructive Evaluation*, vol.20, pp.29-46 (2001)
- [8] Gentzen, V., Choi, Y.-T., Purekar, A.S. & Wereley, N.M., "Experiment Detection and Quantitative Interrogation of Damage in a Jointed Composite Structure", *J. Int. Mat. System and Struct.*, 21 (2010): 275-283.
- [9] Salas, K.I. & Cesnik, C.E.S., "Guided Wave Structural Health Monitoring Using CLoVER Transducers in Composite Materials", *Smart Materials and Structures*, 19 (2010): 1-25.
- [10] K.J. Kirk, A. McNab, A. Cochran, I. Hall and G. Hayward, "Ultrasonic arrays for monitoring cracks in an industrial plant at high temperatures", *IEEE UFFC*, vol.46, no.2, pp. 311-318, (1999)
- [11] P. Kazys, A. Voleisis, and B. Voleisiene, "High temperature ultrasonic transducers: a review", *Ultrasonics*, vol.63, pp.7-17, 2008.
- [12] M. Kobayashi and C.-K. Jen, "Piezoelectric thick bismuth titanate/PZT composite film transducers for smart NDE of metals", *Smart Materials and Structures*, vol.13, 951-956 (2004).
- [13] M. Kobayashi, C.-K. Jen, J.F. Bussiere, and K.-T. Wu, "High temperature integrated and flexible ultrasonic transducers for non-destructive testing", *NDT&E Int.*, vol.42, no.2, pp.157-161, 2009.
- [14] D. H. Wang and S. L. Huang, "Health monitoring and diagnosis for flexible structures with PVDF piezoelectric film sensor array", *Journal of Intelligent Mat. Systems and Structures*, vol. 11, no.6, pp. 482-491, 2000.
- [15] J.-M. Park, J.-W. Kong, D.-S. Kim, and D.-J. Yoon, "Nondestructive damage detection and interfacial evaluation of single-fibers/epoxy composites using PZT, PVDF and P(VDF-TrFE) copolymer sensors", *Composites Science and Technology*, vol. 65, pp. 241-256, 2005.
- [16] A. C. S. Parr, R. L. O'leary and G. Hayward, "Improving the thermal stability of 1-3 piezoelectric composite transducers", *IEEE Trans. Ultrason., Ferroelect., Freq. Contr.*, vol. 52, no. 4, pp. 550-563, 2005.
- [17] C.R. Bowen, L.R. Bradley, D.P. Almond and P.D. Wilcox, "Flexible piezoelectric transducer for ultrasonic inspection of non-planar components", *Ultrasonics*, vol.48, pp.367-375, 2008.
- [18] G. Harvey, A. Gachagan, J.W. Mackersie, T. McCunnie and R. Banks, "Flexible ultrasonic transducers incorporating piezoelectric fibers", *IEEE Trans. Ultrason. Ferroelect. Freq. Control*, vol.56, no.9, pp. 1999-2009, 2009.
- [19] M. Kobayashi, C.-K. Jen and D. Lévesque, "Flexible ultrasonic transducers," *IEEE Trans. UFFC*, vol.53, no.8, pp.1478-1485, 2006.
- [20] D. A. Barrow, T. E. Petroff, R. P. Tandon, and M. Sayer, "Characterization of thick lead zirconate titanate films fabricated using a new sol gel based process", *J. Appl. Phys.*, vol. 81, no. 2, pp. 876-881, 1997.
- [21] I.A. Viktorov, [*Rayleigh and Lamb waves*], Plenum, New York (1967).
- [22] G.S. Kino, [*Acoustic Waves, Devices, Imaging & Analog Signal Processing*], Prentice-Hall, New Jersey (1987).
- [23] C.-K. Jen, Y. Ono and M. Kobayashi, "High temperature integrated ultrasonic shear wave probes", *Applied Phys. Lett.*, vol.89, 183506_1-3 (2006).
- [24] D.W. Greve, H. Sohn, C.P. Yue and I.J. Oppenheim, "An inductively coupled lamb wave transducer", *IEEE Sensors J.*, vol.7, 295-301 (2007).
- [25] K.-T. Wu, M. Kobayashi and C.-K. Jen, "Integrated high temperature piezoelectric plate acoustic wave transducers using mode conversion", *IEEE Trans. UFFC*, vol.56, 1218-1224 (2009).
- [26] G. Velu, D. Remiens and B. Thierry, "Ferroelectric properties of PZT thin films prepared by sputtering with stoichiometric single oxide target: comparison between conventional and rapid thermal annealing", *J. European Ceram. Soc.*, vol. 17, pp. 1949 – 55, 1997.
- [27] H. Hu, C.J. Peng and S.B. Krupanidhi, "Effects of heating rate on the crystallization behaviour of amorphous PZT thin films", *Thin Solid Films*, vol.223, no.2, pp. 327-333, 1993.
- [28] J. Lu, Y. Zhang, T. Ikehara, R. Maeda and T. Mihara, "Effects of rapid thermal annealing on nucleation, growth, and properties of lead zirconate titanate films", *IEEE Trans. UFFC*, vol.54, no.12, pp. 2548- 2554, 2007.
- [29] W.F. Walker and G.E. Trahey, "A fundamental limit on delay estimation using partially correlated speckle signals," *IEEE Trans. Ultrason. Ferroelect. Freq. Control*, vol.42, no. 2, pp.301-8, 1995.
- [30] J.-D. Aussel and J.-P. Monchalain, "Precision laser-ultrasonic velocity measurement and elastic constant determination," *Ultrasonics*, vol.27, no.3, pp.165-177, 1989